The Relationship between Tropical Cyclone Intensity Change and the Strength of Inner-Core Convection

HAIYAN JIANG

Department of Earth and Environment, Florida International University, Miami, Florida

(Manuscript received 23 May 2011, in final form 6 November 2011)

ABSTRACT

Convective intensity proxies measured by the Tropical Rainfall Measuring Mission (TRMM) Microwave Imager (TMI), Precipitation Radar (PR), and Visible and Infrared Scanner (VIRS) are used to assess the relationship between intense convection in the inner core and tropical cyclone (TC) intensity change. Using the cumulative distribution functions of 24-h intensity changes from the 1998–2008 best-track data for global TCs, five intensity change categories are defined: rapidly intensifying (RI), slowly intensifying, neutral, slowly weakening, and rapidly weakening. TRMM observations of global TCs during 1998–2008 are used to generate the distributions of convective properties in the storm's inner-core region for different storm intensity change categories. To examine the hypothesis of hot towers near the eye as an indicator of RI, hot towers are defined by precipitation features with 20-dBZ radar echo height reaching 14.5 km.

The differences in the convective parameters between rapidly intensifying TCs and slowly intensifying, neutral, slowly weakening, and rapidly weakening TCs are quantified using statistical analysis. It is found that statistically significant differences of three out of four convective intensity parameters in the inner core exist between RI and non-RI storms. Between RI and slowly intensifying TCs, a statistically significant difference exists for the minimum 11-μm IR brightness temperature T_{B11} in the inner core. This indicates that a relationship does exist between inner-core convective intensity and TC intensity change. The results in this study also suggest that the rate of intensification appears to be influenced by convective activity in the inner core and the ability to predict RI might be further improved by using convective parameters. With regard to different convective proxies, the relationships are different. The minimum T_{B11}, upper-level maximum radar reflectivities, and maximum 20-dBZ radar echo height in the inner core are best associated with the rate of TC intensity change, while the minimum 85-GHz polarization corrected brightness temperature (PCT) shows some ambiguities in relation to intensity change. The minimum 37-GHz PCT shows no significant relationship with TC intensity change, probably because of the contamination of the ice scattering signal by emission from rain and liquid water in this channel.

By examining the probability of RI for each convective parameter for which statistically significant differences at the 95% level were found of RI and non-RI cases, it is found that all three parameters provide additional information relative to climatology. The most skillful parameter is minimum T_{B11}, and the second is maximum 20-dBZ height, followed by minimum 85-GHz PCT. However, the increases of RI probability from the larger sample mean by using these predictors are not very large.

When using the existence of hot towers as a predictor, it is found that the probabilities of RI and slowly intensifying increase and those of slowly weakening and rapidly weakening decrease for samples with hot towers in the inner core. However, the increases for intensifying and decreases for weakening are not substantial, indicating that hot towers are neither a necessary nor a sufficient condition for RI.

1. Introduction

One of the critical questions in tropical cyclone (TC) research is what the necessary and sufficient conditions are for TC intensification, and especially rapid intensification (RI). Favorable large-scale environmental conditions that are near-universally agreed to be necessary for TC intensification include the following: warm sea surface temperature (SST), high low- to midlevel moisture, and low vertical wind shear (Gray 1968; Merrill 1988). Kaplan and DeMaria (2003) defined RI as the 95th percentile of all 24-h overwater intensity changes, corresponding to approximately 15.4 m s^{-1} (30 kt) or greater.

Corresponding author address: Dr. Haiyan Jiang, Department of Earth and Environment, Florida International University, 11200 SW 8th St., PC-342B, Miami, FL 33174.
E-mail: haiyan.jiang@fiu.edu

DOI: 10.1175/MWR-D-11-00134.1

They used 12-yr TC best track and Statistical Hurricane Intensity Prediction Scheme (SHIPS; DeMaria and Kaplan 1994, 1999) database to study the large-scale characteristics of RI storms in the North Atlantic basin. Besides warmer SST, higher moisture, and lower vertical wind shear, they also found that RI cases are farther from their maximum potential intensity, a parameter closely related to SST, than the non-RI cases. Using the Navy Operational Global Atmospheric Prediction System (NOGAPS) data, Hendricks et al. (2010) studied the environmental control on intensity changes, including rapidly intensifying, intensifying, neutral, and weakening, of 2003–08 TCs in the western North Pacific and North Atlantic basins. They found that SSTs and other environmental parameters of RI TCs and intensifying TCs are quite similar, indicating that the rate of intensification is only weakly dependent on the environmental conditions, on average. Therefore they argued that the RI is more likely controlled by internal dynamical processes, provided that a preexisting favorable environment exists. However, Kaplan et al. (2010) demonstrated that it is possible to make skillful RI forecasts while utilizing only large-scale environmental parameters. This implies that both environment and storm internal processes are playing a crucial role in RI.

The sufficient conditions of TC intensification, and in particular, RI, are still controversial. Precipitation in the inner-core region is closely related to the latent heat release and the internal process of the development of a storm. Rao and MacArthur (1994) found that rain rates averaged in the 2.0° radius box were highly correlated with 24-h future typhoon intensity. Cecil and Zipser (1999) examined TCs in the Atlantic, eastern North Pacific, and western North Pacific observed by the Special Sensor Microwave Imager (SSM/I) during 1995 and 1996. The inner-core areal mean 85-GHz polarization corrected brightness temperature (PCT; an indicator of ice scattering; Spencer et al. 1989) and the average area of 85-GHz PCT less than 250 K were found to be highly correlated (correlation coefficients around -0.7) with the future hurricane/typhoon intensity. As pointed out by Spencer et al. (1989) the 250-K PCT is considered as an indicator of moderate rain rate. Therefore, the results from Cecil and Zipser (1999) indicate that the strongest correlations involve the spatial coverage of at least moderate inner-core precipitation rates. Similarly, Kerns and Zipser (2009) found that enhanced TC genesis probability is associated with greater cold cloud area and raining area, especially in the eastern North Pacific.

The above-mentioned parameters that produce the highest correlations with intensity respond primarily to the mesoscale nature of the precipitation, as opposed to the convective scale. A recent debate has been focused on the possible role of intense convective events. Hot towers (Simpson et al. 1998) and convective bursts (Steranka et al. 1986) near the storm center were found to be related to TC intensification. Kelley et al. (2004, 2005) found that the chance of TC intensification increases when one or more hot towers exist in the eyewall. Hendricks et al. (2004) and Montgomery et al. (2006) proposed that intense ''vortical hot towers'' may be a missing link in the chain of events that transforms a midlevel vortex into a near-surface vortex, initiating TC genesis and RI. Vigh and Schubert (2009) found that the warm core in TCs may rapidly develop if a portion of the deep convection occurs in the inner-core region. Rogers (2010) and Guimond et al. (2010) also emphasize the importance of hot towers and convective bursts near the eye in TC rapid intensification.

The purpose of this study is to objectively quantify the relationship between convective intensity in the inner-core region and the TC intensity change, and in particular, RI. Using the best-track cumulative distribution functions of 24-h intensity changes from 1998 to 2008, we define five separate intensity change categories for global TCs: 1) rapidly intensifying, 2) slowly intensifying, 3) neutral, 4) slowly weakening, and 5) rapidly weakening. Then the Tropical Rainfall Measuring Mission (TRMM) satellite-based Tropical Cyclone Precipitation Feature (TCPF) database (Jiang et al. 2011) is used to create a dataset including convective intensity proxies in the inner-core region of TCs for each intensity categories. Generally the convective intensity is defined by updraft magnitude. Since it is impossible for satellites to measure the updraft speed in a storm, many studies used convective proxies derived from radar, microwave radiometer, lightning, and IR sensors (Cecil et al. 2005; Zipser et al. 2006; Liu et al. 2007). We adopt the same view in this study. The convective intensity proxies used here include vertical profile of radar reflectivity, minimum IR brightness temperature at 10.8-μm channel (T_{B11}), and minimum 85- and 37-GHz PCT observed by TRMM. Using the dataset, we will show the convective characteristics that differentiate rapidly intensifying versus slowly intensifying, as well the convective characteristics that differentiate intensifying versus weakening TCs. Additionally the probability of RI will be estimated for samples meeting the hot tower definition, which is that maximum 20-dBZ radar echo $\geq$14.5 km. The key questions to be addressed are the following: 1) Is the convective intensity near the storm center related to TC intensification and rapid intensification? 2) How much information do convective indicators provide for RI forecasts? 3) Is a hot tower a sufficient or necessary condition for RI? In section 2, the data and methods for the study are described. In section 3, the distributions

of convective proxies are presented to examine the relationship between convective intensity and TC intensity change. In section 4, the probability of RI is estimated by using TRMM-derived convective properties and hot towers in the inner-core region as predictors. Finally, the main conclusions of this study are given in section 5.

2. Data and methods

a. TRMM TCPF data

The Florida International University (FIU) and University of Utah (UU) TRMM TCPF database (Jiang et al. 2011) is built upon the UU TRMM precipitation feature (PF) database, which is based on the framework of PFs that were defined by grouping contiguous pixels based on certain criteria as observed by TRMM (Nesbitt et al. 2000; Liu et al. 2008). A variety of different criteria are used to define PFs. For example, Nesbitt et al. (2000) selected contiguous areas with near-surface reflectivity equal or greater than 20 dBZ or 85-GHz PCT equal or less than 250 K as PFs. The PF definition used in this study is the TRMM Precipitation Radar (PR) rainfall product 2A25 (Iguchi et al. 2000) near-surface rain rate greater than zero. The TCPF database includes all PFs that are associated with TCs. To be qualified as a TCPF, the distance between the TC center and the PF center has to be less than 500 km. Here the PF center is a raw geometric center, and the TC center for each TRMM observation is interpolated from the best-track data, which are obtained from National Hurricane Center (NHC) for the Atlantic and eastern North Pacific basins, and from the Joint Typhoon Warning Center (JTWC) for all other TC-prone basins. A series of storm parameters are calculated from the best-track information. The storm parameters that are used in this study include the following: land/ocean flag of TC center at the time of TRMM observation and 6-, 12-, 18-, and 24-h future; storm 24-h future intensity change; and the current and 6-, 12-, 18-, and 24-h future flag of extratropical transition (ET). The ET flag is from best-track data. The level 2 of TRMM TCPF data also includes the statistical parameters from measurements and retrievals from TRMM Microwave Imager (TMI), PR, and Visible and Infrared Scanner (VIRS), and Lightning Imaging System (LIS). Specific details of parameters available in each TCPF in level-2 data and collocation methods can be found in Liu et al. (2008) and Jiang et al. (2011). The convective intensity proxies used in this study are selected from these parameters (see section 2b).

b. Selection of TRMM overpasses, PFs, and convective parameters

The TRMM TCPF data used in this study were collected for the period 1998–2008. A total of 945 TCs that reached tropical storm intensity level or above are included in the FIU/UU TRMM TCPF database for 1998–2008. This includes over 13 000 TRMM TC overpasses. Because of the limited swath width of TRMM PR (215 km wide before TRMM boost in August 2001 and 247 km after boost), not all TRMM TC overpasses captured the storm in full. Since this study concerns the convective intensity in the inner-core region, we first manually filter the overpasses so that only those that captured all or most of the inner-core region are included. The inner-core region is the eyewall region for strong TCs with an eye. The eyewall is a circular band of convection and precipitation that encircles the eye. In the cases of low-intensity TCs without a clear eye (therefore no eyewall), near-center convection is identified and included in the inner-core region. Therefore, the inner-core region includes complete eyewalls, imcomplete or partial eyewalls, concentric eyewalls, and near-center convection for storms without an eye. In this study, the inner-core region and the outermost radius of inner-core convection are *subjectively* determined by looking at the horizontal fields of TRMM radar reflectivity and TMI 85-GHz ice scattering. An approach similar to Cecil et al. (2002) is used to make the outer boundary of the inner-core region at the outer edge of the horizontal gradient of reflectivity or ice scattering. About 1600 overpasses that captured all or most of the inner-core region are selected. Figure 1 shows an example of selected TRMM overpasses (Hurricane Isaac in 2006). In this case, hot towers are found within the outermost radius of the inner core.

Next, similar to the methodology used Kaplan and DeMaria (2003) and Hendricks et al. (2010), for overpasses to be included in the selected sample, the storm has to be remained over water within a +24-h period. Both mainland and island interactions are removed. Finally, overpasses where the TC underwent ET within +24 h are removed. The filtered dataset yield 1076 TRMM TC overpasses with valid 24-h intensity change values, and no missing data for the selected convective parameters listed below. The geographic distribution of the 1076 TRMM TC overpasses is given in Fig. 2.

For most of TC overpasses, precipitation features associated with the inner-core convection (i.e., eyewall for stronger storms) are naturally separated from features associated with rainbands. However, there are some cases in which only one large PF exists for the whole TC region. To define the inner-core regions, the outermost radius of inner-core convection is used to separate inner-core PFs from rainbands. Then for each overpass, only the most convectively intense inner-core PF is selected using the PR maximum 20-dBZ echo height as a criterion. The minimum PF size threshold of 75 km^2 is applied, too.

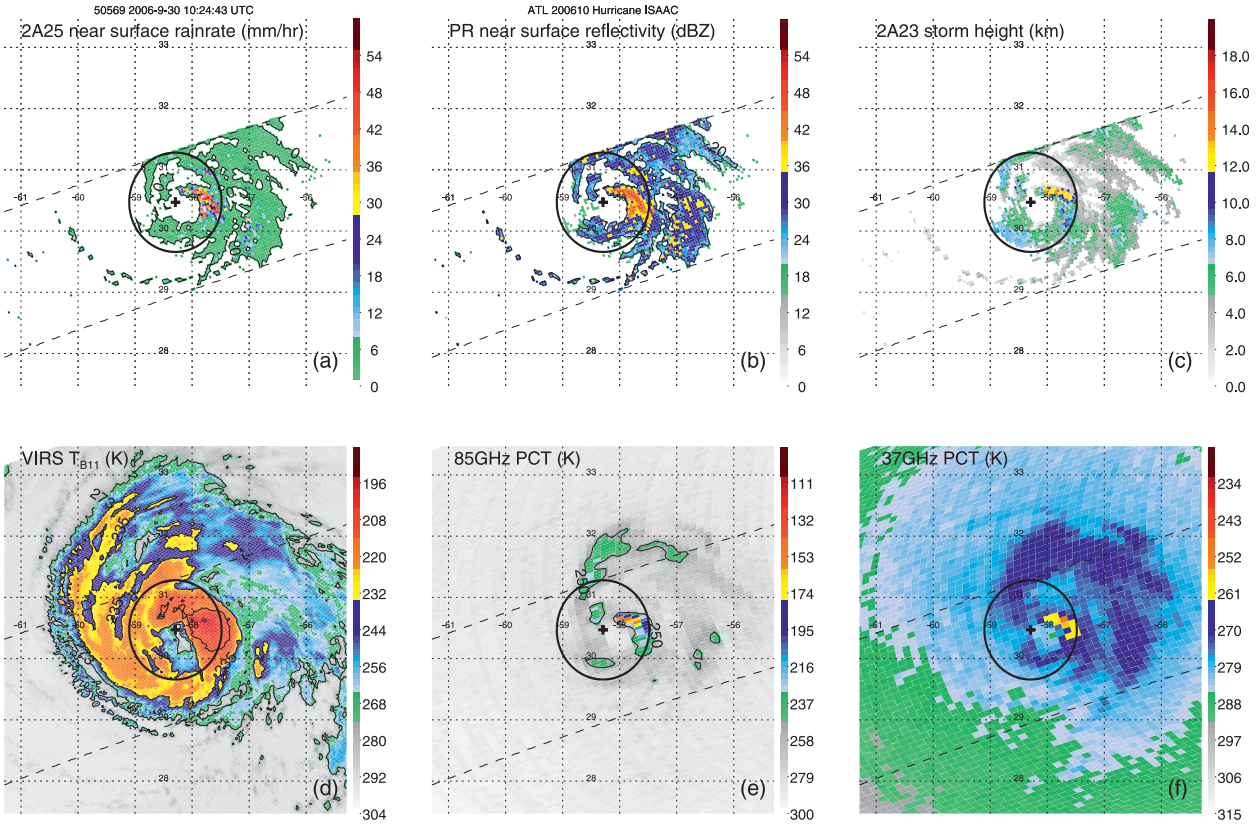

FIG. 1. Examples of (a) PR 2A25 near-surface rain rate (mm h^{-1}), (b) PR near-surface reflectivity (dBZ), (c) PR 2A23 storm height (km; Awaka et al. 1998), (d) VIRS T_{B11} (K), (e) TMI 85-GHz PCT (K), and (f) TMI 37-GHz PCT (K) from Hurricane Isaac, TRMM orbit 50569, at 1024 UTC 30 Sep 2006. The cross at the center of (a)–(f) is the hurricane center location. The circle in each indicates the outermost radius of inner-core convection. The dashed line in each is the edge of the PR swath.

For the most convectively intense PF in each of the 1076 selected overpasses, the maximum radar reflectivity profile, maximum 20-dBZ echo height, minimum T_{B11}, minimum 85- and 37-GHz PCT are used as proxies of convective intensity of the inner-core region of TCs. These are all point measures of convective intensity, which are meant to represent the strongest convection within the inner-core region. The maximum radar reflectivity as a function of altitude depends on the size, phase, and concentration of the largest precipitation particles at specific vertical levels. Below the freezing level, high reflectivity values indicate high liquid water content and rain rate. Above the freezing level in the mixed phase region, typically 6–9 km, the high reflectivity values are indicative of supercooled liquid raindrops or large ice hydrometeors produced by substantial convective updrafts. In the absence of strong updrafts, reflectivity decreases rapidly with height above the freezing level. Above about 9-km altitude, higher reflectivity values indicate stronger updrafts. Therefore, the maximum 20-dBZ echo height is an indicator of storm height and is related to the strength of upper-level updrafts.

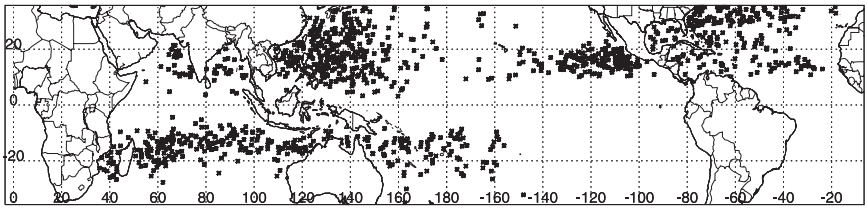

FIG. 2. Geographic distribution of the 1076 selected TRMM TC overpasses (please see text for details).

The traditional way to define deep convection is to use the cloud-top temperature measured by IR brightness temperature T_B. The major limitation of IR T_B as a convective intensity proxy is related to the anvil contamination. Since here the PF is grouped by the PR 2A25 near-surface rain rate greater than zero, the anvil contamination is eliminated. The minimum T_{B11} here indicates how high a convective cloud in the inner-core region can reach. The cold cloud-top height indicated by this parameter is always higher than maximum 20-dBZ radar echo height for the same feature. This parameter is related to both the convective intensity and the level of neutral buoyancy, or tropopause height (Liu et al. 2007). The microwave brightness temperatures at 85 and 37 GHz respond to scattering of upwelling radiation by precipitation-sized ice particles, which reduce the observed brightness temperature. However, the low brightness temperature due to ice scattering could be confused with the sea surface, which also appears cold due to low sea surface emissivity in 85- and 37-GHz channels. The PCT at 85 GHz (Spencer et al. 1989) and 37 GHz (Cecil et al. 2002) is defined to remove the ambiguity in such a way that PCTs are cold for ice scattering and warm for the sea surface regions. The minimum 85- and 37-GHz PCT depends on the optical path of large frozen hydrometeors. This is similar to a column-integrated ice mass weighted toward larger particles, especially at 37 GHz, with its longer wavelength (Vivekanandan et al. 1991). The minimum PCT generally represents the deepest, most vigorous convection in the storm. However, it should be noted that emission by liquid water also contributes to higher PCTs at these frequencies, especially at 37 GHz.

c. Selection of intensity change categories

To find an RI threshold for TCs during 1998–2008, a procedure similar to Kaplan and DeMaria (2003) is used. As in the TCPF database, TCs that reached tropical storm intensity level or above are included in the analysis. Using the 6-hourly best-track data, +24-h (24 h into the future) intensity changes are calculated and recorded at each 0000, 0600, 1200, and 1800 UTC synoptic time. Cases with land interaction and undergoing ET are removed. The probability density function (PDF) and cumulative distribution function (CDF) for these data are shown in Fig. 3. There are three extreme rapidly intensifying events with 24-h intensity changes between 43.7 m s^{-1} (85 kt) and 48.9 m s^{-1} (95 kt). They are associated with Hurricane Wilma (2005) and Hurricane Felix (2007) in the North Atlantic basin, and Typhoon Chebi (2006) in the northwest Pacific basin. There are two extreme rapidly weakening events with 24-h intensity changes of −43.7 m s^{-1} (−85 kt) and −46.3 m s^{-1} (−90 kt). Both of these events are associated with Super Typhoon Damrey (2000). The 95th percentile of the CDF is 15.8 m s^{-1} (30.8 kt). An RI threshold of 43.7 m s^{-1} (30 kt) is employed in this study since it is in better agreement with the 30.84-kt threshold than the next closest 24-h intensity change of 35 kt due to the 5-kt resolution of the best-track data. Four more intensity change categories are defined using equal-sized bins. Using the criterion for each category, the 1076 TRMM overpasses are separated into five intensity change categories: rapidly intensifying, slowly intensifying, neutral, slowly weakening, and rapidly weakening. Table 1 lists the five intensity change categories, along with the range and sample size.

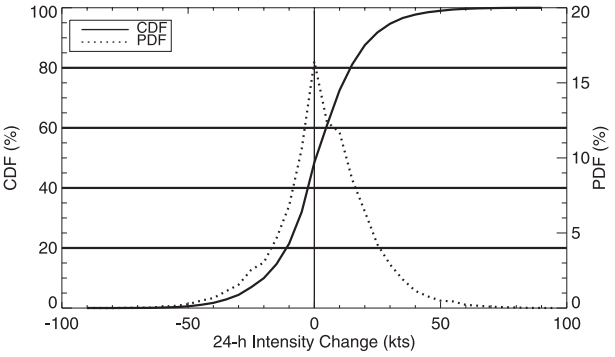

FIG. 3. Probability density and cumulative distribution functions for 24-h overwater intensity changes of global TCs during 1998–2008.

The RI sample employed in this study comprises 64 TCs compared with the sample total of 811 TCs (Table 1). These 64 TCs contributed a total of 68 RI samples since it is possible for a TC to undergo RI more than once during its lifetime. Similarly, for other intensity change groups, there are also a small percentage of samples that are not unique.

Table 2 shows the distribution of the different intensity change samples as a function of the initial TC intensity. The table shows that systems that are initially of tropical storm intensity account for the largest percentage of RI cases while category 1–2 hurricanes contribute the next largest percentage, tropical depressions the third largest percentage, and category 3–5 hurricanes the smallest percentage. This is consistent with Kaplan et al. (2010), which showed that tropical storms compose the highest percentage for RI cases in Atlantic and eastern North Pacific basins. Only 2 out of 68 RI cases are from TCs initially at category 3–5 hurricane intensity stage. In contrast, only 1 out of 26 rapidly weakening cases are from tropical storms or tropical depressions. A majority of rapidly weakening cases are from hurricanes. The average maximum surface wind speed of rapidly weakening storms (93 kt) is about a factor of 2 higher than that of rapidly intensifying storms (52 kt; Table 2).

TABLE 1. Definitions of intensity change categories. The number of TRMM overpasses and number of TCs for each category. ΔV_{max24} represents the maximum sustained wind change within the next 24 h; 1 kt = 0.5144 m s^{-1}.

Category	Max wind speed range (kt)	No. of TRMM overpasses	No. of TCs
RW	$\Delta V_{max24} < -30$	26	25
SW	$-30 \le \Delta V_{max24} < -10$	114	98
N	$-10 \le \Delta V_{max24} < 10$	535	355
SI	$10 \le \Delta V_{max24} < 30$	333	269
RI	$\Delta V_{max24} \ge 30$	68	64
Tot		1076	811

3. Convective properties associated with TC intensity change

The dataset we construct here contains only the point measure of the most intense convective intensity in the inner-core region. In this section, the distributions of convective intensity for different TC intensity change categories are compared.

a. Maximum radar reflectivity profile

The vertical profile of maximum radar reflectivity is often a strong indicator of storm or convective intensity (Szoke and Zipser 1986; Zipser and Lutz 1994; Cecil et al. 2005). The higher the reflectivity in and above the mixed-phase region is, the more intense the convection tends to be. Figure 4 shows the vertical profiles of maximum radar reflectivity for RI versus other intensity change groups. At upper-level above 11 km for the 30th percentile (Fig. 4a), above 13 km for the median profiles (Fig. 4b), and above 14 km for the 70th percentile (Fig. 4c), the maximum reflectivity in the inner core of RI storms is the highest, and that for slowly intensifying storms is the second highest. For the median profiles (Fig. 4b), at 17 dBZ, which is the minimum PR detectable reflectivity value, RI storms reach 14.5 km, slowly intensifying storms reach 13.5 km, slowly weakening storms reach 11.5 km, while neutral and rapidly weakening storms reach 12.5 km. This suggests that the median maximum storm height in the inner core decreases moving from RI to slowly intensifying to neutral to slowing weakening storms. However, rapidly weakening storms have higher medium maximum storm height than slowly weakening storms. For the 90th percentile (Fig. 4d), above 15-km altitude, the maximum reflectivity of RI storms overlaps with slowly intensifying storms and is higher than that for neutral, slowly weakening, and rapidly weakening storms. It is noticed that for rapidly weakening storms, the 90th percentile of the maximum reflectivity profile in the inner-core region only reaches 14 km, which is 2–3-km lower than other intensity change groups. Considering all four percentiles shown in Fig. 4, it is suggested that RI storms have the strongest updrafts in the upper-level of the inner-core region, with slowly intensifying the second, neutral the third, slowly weakening the fourth, and rapidly weakening the weakest.

In the mixed-phase region (between 6 and 11 km for different percentiles), the slope of maximum reflectivity profiles in the inner-core region are quite similar for different intensity change groups, except that the reflectivity decreases with height more sharply for rapidly weakening storms than other groups. Note that the reflectivity values are the highest for rapidly weakening storms at 5–6 km for all four percentiles (Figs. 4a–c), but decrease sharply with height and become the smallest at 11 km in 70th and 90th percentiles (Figs. 4c,d) and the third smallest (greater than those for neutral and slowly weakening groups) at 11 km for 30th and 50th percentiles (Figs. 4a,b). As mentioned in section 2b, the rapid decrease of reflectivity with height indicates the absence of strong updrafts above the freezing level.

At levels below 5 km, rapidly weakening storms in the inner-core region have the highest reflectivity values for the 30th, 50th, 70th, and 90th percentiles (Figs. 4a–d). The RI storms have the lowest reflectivity for the 90th percentile (Fig. 4d), which is just slightly lower than those for slowly intensifying and neutral storms. Slowly weakening storms have the second highest reflectivity for the 90th percentile. At the 30th, 50th, and 70th percentiles (Figs. 4a–c), the order of reflectivity values in lower level

TABLE 2. The distribution of different intensity change samples as a function of intensity class and the average maximum surface wind speed (Vmax, kt) for different intensity change groups; 1 kt = 0.5144 m s^{-1}.

Category	Tropical depression (TD)	Tropical storm (TS)	Category 1–2 hurricane (CAT12)	Category 3–5 hurricane (CAT35)	Tot cases (%)	Avg Vmax (kt)
RW	1	1	12	13	26 (2.4)	93
SW	4	52	31	27	114 (10.6)	73
N	235	195	75	30	535 (49.7)	45
SI	153	123	42	15	333 (30.9)	43
RI	16	31	19	2	68 (6.3)	52
Tot cases (%)	408 (38)	402 (37)	179 (17)	87 (8)	1076 (100)	49

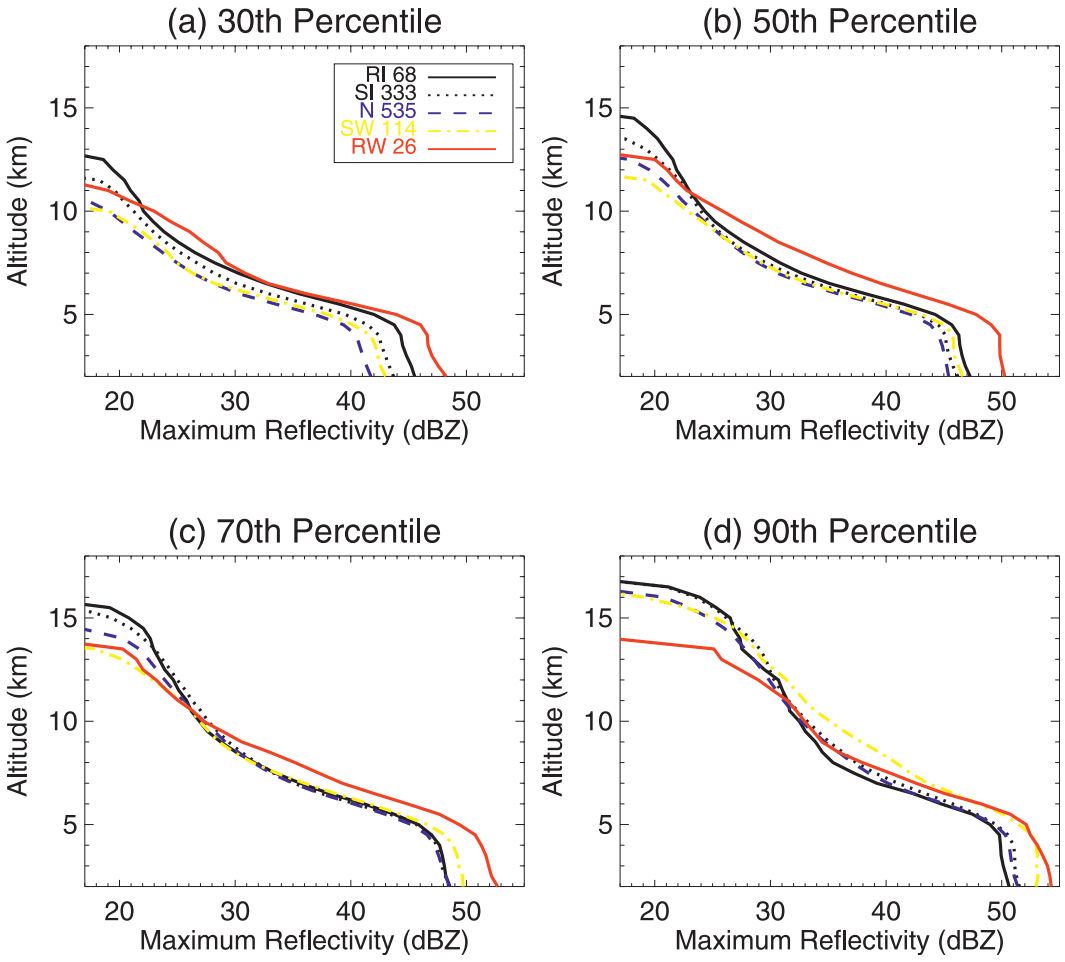

FIG. 4. The (a) 30th, (b) 50th, (c) 70th, and (d) 90th percentiles of maximum radar reflectivity as a function of height for the most convectively intense PFs in the inner-core region of TCs in different intensity change stages: rapidly intensifying (RI), slowly intensifying (SI), neutral (N), slowly weakening (SW), and rapidly weakening (RW).

of the inner-core region varies among different intensity change groups, although rapidly weakening storms remain the highest. As indicated in section 2b, high reflectivity below the freezing level indicates high liquid water content and rain rate. Therefore, Fig. 4 indicates that RI storms have the strongest updraft in the upper level, but produce lower liquid water content and surface rain rate. In contrast, rapidly weakening storms produce the highest liquid water content and rain rate in the lower level and surface, but have the weakest updraft in the middle level and weaker updraft in the upper level. It is not surprising that rapidly weakening storms produce the strongest surface rain in the inner-core region. From section 2c and Table 2, we can see that these storms are mainly storms with high initial/current intensity. Figure 5 shows the mean and median profiles of maximum reflectivity for the most convectively intense PFs in the inner-core region for storms in different current intensity stages. We can see that hurricanes have much higher reflectivity values in all altitudes, especially in lower levels, than tropical storms and depressions.

b. *Minimum brightness temperatures and maximum 20-dBZ echo height*

The CDFs of other convective proxies in the inner-core region, including minimum 10.8-μm brightness temperature T_{B11} observed by VIRS, maximum 20-dBZ echo height observed by PR, and minimum 85- and 37-GHz PCT observed by TMI are compared for different intensity change categories (Fig. 6). The RI storms have higher (colder) cloud tops in the inner-core region than slowly intensifying storms, which have higher cloud tops than neutral and slowly weakening storms over the whole convective spectrum. Rapidly weakening storms have the highest cloud-top height at the warmest end (between 95% and 100% frequency in Fig. 6a) of the

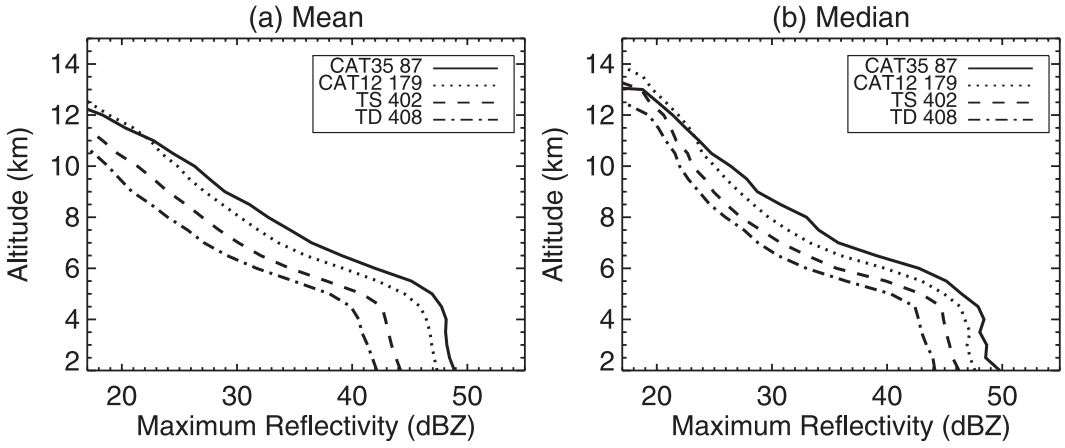

FIG. 5. (a) Mean and (b) median profiles of maximum radar reflectivity for the most convectively intense PFs in the inner-core region of TCs in different intensity categories: RI, SI, N, SW, and RW.

minimum T_{B11} distribution, and the lowest cloud-top height at the coldest end (between 0% and 20% frequency in Fig. 6a) of the minimum T_{B11} distribution. The different behavior of rapidly weakening storms is mainly due to the higher initial storm intensity of this group. The range of minimum T_{B11} values is 185–210 K for rapidly weakening storms, 174–223 K for RI storms, and 171–280 K for all other intensity change storms. Figure 6a shows that the fraction of RI cases increases for low minimum T_{B11} values with nearly 70% of all RI storms having minimum T_{B11} less than 190 K compared with only 60% of slowly intensifying cases, 40% of neutral cases, and 30% of slowly and rapidly weakening cases. Without considering rapidly weakening cases, a good

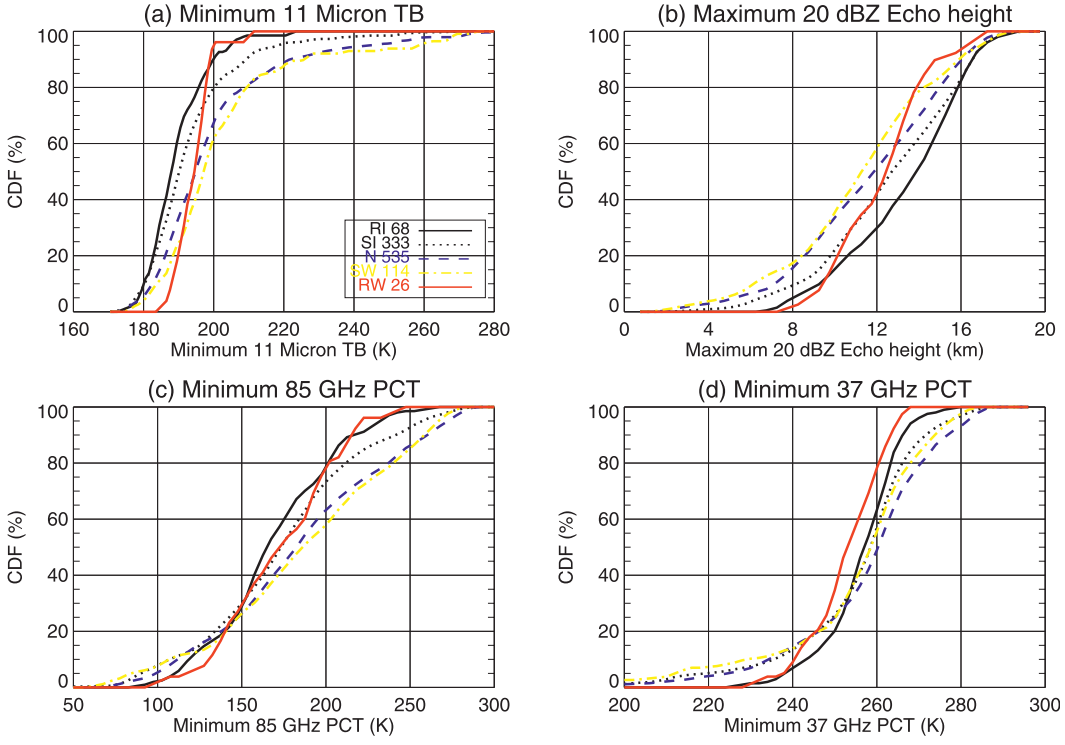

FIG. 6. CDFs of (a) minimum 11-μm T_B, (b) maximum 20-dBZ echo height, (c) minimum 85-GHz PCT, and (d) minimum 37-GHz PCT for the most convectively intense PFs in the inner-core region of TCs in different intensity change stages: RI, SI, N, SW, and RW.

relationship is seen between the rate of TC intensification and the mean and median cloud-top heights in the inner-core region.

Similarly, substantial differences among the distributions of maximum 20-dBZ echo height of different intensity change groups are seen (Fig. 6b). Over the whole spectrum, RI storms have higher maximum 20-dBZ echo height in the inner core than slowly intensifying storms, which have higher maximum 20-dBZ echo height than neutral and slowly weakening storms. Again, the rapidly weakening group behaves differently due the reason stated above. Specifically, 70% of RI storms occurred when the maximum 20-dBZ echo height in the inner-core region is greater than 12 km (the total study sample of the mean maximum 20-dBZ echo height is 12.1 km) compared to 60% of slowly intensifying and rapidly weakening cases, 50% of neutral cases, and 40% of slowly weakening cases. It is also interesting to notice that the minimum maximum 20-dBZ echo height is 7–8 km in order for RI or rapidly weakening cases to occur. This minimum value is much smaller (2–4 km) for all other intensity change categories. This indicates that the necessary condition for a rapid intensity change to occur is that the storm height in the inner-core region has to be high enough, consistent with the minimum T_{B11} ranges shown in Fig. 6a.

Differences among the distributions of ice scattering signatures in the inner-core region of different intensity change groups are not very obvious (Figs. 6c,d), especially for 37-GHz PCT (Fig. 6d). At the strongest end of convective spectrum (top 20% or minimum 85-GHz PCT less than about 140 K), the 85-GHz ice scattering signatures, as indicated by minimum 85-GHz PCT, in slowly weakening, slowly intensifying, and, neutral storms are stronger than those in RI and rapidly weakening storms (Fig. 6c). At middle of convective spectrum (between top 20% and 90% or minimum 85-GHz PCT between 140 and 210 K), 85-GHz ice scattering signatures near the storm center of RI storms are stronger than those in slowly intensifying, rapidly weakening, neutral, and slowly weakening storms. At the weakest end of convective spectrum (bottom 10% or minimum 85-GHz PCT warmer than 210 K), 85-GHz ice scattering signatures in the inner-core region of rapidly weakening storms are stronger than those in RI, slowly intensifying, neutral, and slowly weakening storms. Again, this suggests, although with some ambiguities, a good relationship between 85-GHz ice scattering signature and the rate of TC intensification when excluding the rapidly weakening group. It is also interesting to see that the minimum 85-GHz PCT in the inner-core region must be colder than 250 K in order for RI or rapidly weakening cases to occur. This minimum value is much higher ($\sim$280 K) for all other intensity change categories. This is similar to the necessary condition of cloud/radar echo top height for a rapid intensity change to occur.

Similar to 85-GHz ice scattering signatures, distributions of minimum 37-GHz PCT in the inner-core region show mixed pictures for the convective intensity difference among different intensity change groups (Fig. 6d). First of all, rapidly weakening storms have lower minimum 37-GHz PCT (stronger ice scattering signature) in the inner-core region than RI storms for the whole convective spectrum. Second, at the strongest end of convective spectrum (top 30% or minimum 37-GHz PCT colder than about 255 K), the 37-GHz ice scattering signatures in slowly weakening, slowly intensifying, and, neutral storms are stronger than those in RI storms (Fig. 6d). At the middle and weakest end of convective spectrum (bottom 70% or minimum 37-GHz PCT warmer than 255 K), 37-GHz ice scattering signatures near the storm center of RI storms are stronger than those in slowly intensifying, slowly weakening, and neutral storms. The mixed picture of 37-GHz ice scattering signature might be due to the contamination of liquid water emission (Spencer et al. 1989) and this channel's sensitivity to larger particles (Vivekanandan et al. 1991).

Above four convective intensity parameters at the start of each of the 68 episodes of RI are compared to those at the beginning of slowly intensifying, slowly weakening, neutral, rapidly weakening, and non-RI (non-RI represents all the slowly intensifying, slowly weakening, neutral, rapidly weakening cases together) cases to determine if the convective intensity parameters for RI samples are significantly different with other groups. Table 3 shows the mean values of the four convective intensity parameters for different intensity change categories. The differences between the mean magnitudes of the RI samples and other categories are also presented in the table. Asterisks are placed beside those differences that are determined to be statistically significant at the 95% level using a two-tailed t test that assumes unequal variances.

Table 3 indicates that statistically significant differences exist between RI and all other intensity change groups for minimum T_{B11} in the inner-core region. The mean value of minimum T_{B11} in the inner-core region is significantly lower for RI cases than that for slowly intensifying, rapidly weakening, neutral, slowly weakening, and non-RI cases. As for the maximum 20-dBZ echo height in the inner-core region, the mean value is significantly higher for RI cases than neutral, slowly weakening, rapidly weakening, and non-RI cases. However, the difference of this value between RI and slowly intensifying cases is not statistically significant, which means that the null hypothesis (i.e., no difference between RI

TABLE 3. The mean values of minimum T_{B11}, maximum 20-dBZ echo height, and minimum 85- and 37-GHz PCT for the most convectively intense PFs in the inner-core region for different intensity change groups: RI, SI, N, SW, RW, and non-RI. The non-RI sample represents all SI, N, SW, and RW samples together. The sample size of each category is shown in the first column. The differences for each quantity between RI and other categories are shown in the last five rows; asterisk denotes statistical significance at the 95% level.

	Sample size	Min T_{B11} (K)	Max 20-dBZ echo height (km)	Min 85-GHz PCT (K)	Min 37-GHz PCT (K)
RI	68	189.74	13.48	171.00	257.15
SI	333	193.64	12.77	176.03	256.15
N	535	199.95	11.75	186.69	258.36
SW	114	202.63	11.29	188.24	255.61
RW	26	194.68	12.38	174.52	253.36
Non-RI	1008	198.03	12.05	183.03	257.19
RI − SI		−3.9*	0.71	−5.03	1.00
RI − N		−10.21*	1.73*	−15.70*	−1.22
RI − SW		−12.89*	2.19*	−17.24*	1.53
RI − RW		−4.94*	1.09*	−3.53	3.78
RI − non-RI		−8.29*	1.43*	−12.03*	−0.05

and slowly intensifying storms) may be true. The mean value of minimum 85-GHz PCT in the inner-core region is significantly colder for RI storms than that for neutral, slowly weakening, and non-RI storms. But the differences between RI and slowly intensifying and rapidly weakening cases are not significant. For the minimum 37-GHz PCT, none of the differences between RI and other categories is significant.

4. Estimating probability of RI

In this section, estimates of the probability of RI are obtained for each of the three TRMM-observed convective parameters listed in Table 3 for which statistically significant differences were found at 95% level or greater between the RI and non-RI samples. These three parameters are minimum T_{B11}, maximum 20-dBZ echo height, and minimum 85-GHz PCT in the inner-core region. Probabilities are calculated by comparing each of the parameters of the 1076 cases that composed the study sample to the corresponding RI threshold. The methodology used here is the same as that used in Kaplan and DeMaria (2003). The RI threshold for each parameter is defined as the RI sample mean as shown in Table 3. A threshold is said to be satisfied if a value is either $\leq$ or $\geq$ the specific RI threshold. For example, the RI sample has a mean maximum 20-dBZ echo height of 13.5 km. Thus, the maximum 20-dBZ echo height RI threshold is satisfied when the maximum 20-dBZ echo height is $\geq$13.5 km.

Besides using the RI sample mean as the RI threshold, to examine the hypothesis of hot towers near the storm center as an indicator of RI (Simpson et al. 1998; Montgomery et al. 2006), we also estimate the probability of RI when one or more hot towers exist in the inner region. Hot towers are defined by maximum 20-dBZ echo height $\geq$14.5 km by following the definition of Kelley et al. (2004).

Figure 7 shows the probability of RI for each of the three parameters. These probabilities are obtained by dividing the number of RI cases that satisfied a given threshold by the number of cases in the entire sample (1076 cases) that satisfied that same threshold. For example, RI occurred 38 times when the threshold for minimum T_{B11} is satisfied, but the minimum T_{B11} threshold is satisfied a total of 424 times. Thus, the probability of RI is 10.3% (38/424) when the RI threshold for minimum T_{B11} is satisfied. The figure shows that the probability of RI ranges from 7.9% when the threshold for the minimum 85-GHz PCT is satisfied to 10.3% when the threshold for minimum T_{B11} is satisfied. For comparison, the sample mean probability of RI is 6.3% (68 RI cases/1076 total cases). Thus, the probability of RI when an RI threshold is satisfied exceeds the probability of RI when an RI threshold is not satisfied for each of the three predictors (Fig. 7). Also, these RI probabilities are all

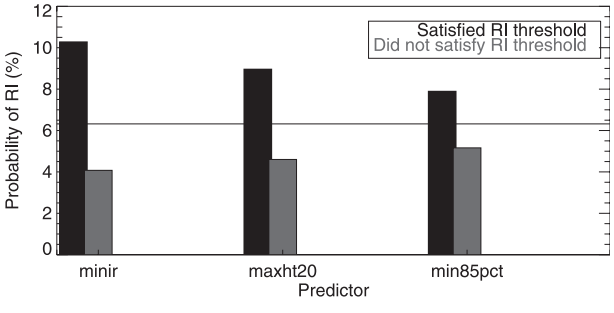

FIG. 7. Probability of RI for predictors satisfying and not satisfying RI thresholds. The predictors include minimum T_{B11} (minir), maximum 20-dBZ echo height (maxht20), and minimum 85-GHz PCT (min85pct). The sample mean (climatological probability of RI) is indicated by the solid line at the 6.3% level.

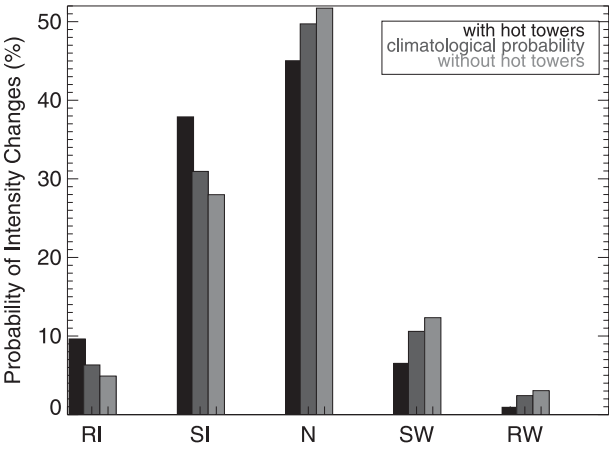

FIG. 8. Probability of RI, SI, N, SW, and RW for the most convectively intense PFs in the inner-core region of TCs with or without hot towers.

larger than the sample mean probability of RI. This suggests that convective intensity parameters do provide additional information over that which is provided by climatology. However, we also notice that the increases of RI probability from the sample mean by using these predictors are not very large, ranging from 1.6% when the RI threshold for minimum 37-GHz PCT is met to 4% when the RI threshold for minimum T_{B11} is met. This indicates that although storm internal processes, such as convective intensity, are important for RI, environmental parameters have to be considered as well in order to improve the prediction of RI (Kaplan et al. 2010).

The probabilities of RI—slowly intensifying, neutral, slowly weakening, and rapidly weakening—are compared for the most convectively intense PFs in the inner-core region of TCs with or without hot towers (Fig. 8 and Table 4). These probabilities are obtained by dividing the number of cases with hot towers that fall in a given intensity change category by the number of cases in the entire sample (1076 cases) that fall in the same intensity change. For example, RI occurred 31 times when one or more hot towers exist (the maximum 20-dBZ echo height $\geq$14.5 km) in the inner-core region, but hot towers are found a total of 322 times. Thus, the probability of RI is 9.6% (31/322) when one or more hot towers exist (Table 4). Figure 8 shows that the probability of RI (slowly intensifying) increases from 4.9% (28.0%) for samples without hot towers, to 6.3% (31.0%) for total sample mean (i.e., climatological probability), and to 9.6% (38.0%) for samples with hot towers in the inner-core region. In contrast, the probability of rapidly weakening (slowly weakening) decreases from 3.1% (12.3%) for samples without hot towers, to 2.4% (10.6%) for total sample mean, and to 0.9% (6.5%) for samples with hot towers in the inner-core region. This suggests that hot towers could be an additional predictor in improving TC intensity change forecasts. However, as we noticed for other convective intensity parameters above, the increases of RI and slowly intensifying probabilities from the sample mean by using the hot tower predictor are not very large, ranging from 3.3% for RI and 7% for slowly intensifying. The probability of RI (slowly intensifying) is still 4.9% (28.0%) for samples without hot towers.

5. Conclusions

Both the storm internal processes and large-scale environmental conditions are controlling factors of tropical cyclone intensity change. This study has been an effort to quantify the relationship between inner-core convective intensity and TC intensification, and in particular rapid intensification. The 11-yr TRMM TCPF database is used to assess the convective characteristics of TCs undergoing different intensity change episodes. A couple of convective proxies are examined to quantify their relationships with TC intensity change. Probabilities of RI are estimated using these convective parameters and the existence of hot towers as predictors.

The differences in the convective parameters between rapidly intensifying TCs and slowly intensifying, neutral, slowly weakening, and rapidly weakening TCs are quantified using statistical analysis. It is found that statistically

TABLE 4. Number of samples with and without hot towers in the most convectively intense PF in the inner-core region for different intensity change groups: RI, SI, N, SW, and RW. The probabilities of intensity changes for samples with and without hot towers for each intensity change category is also shown, and compared with the climatological probabilities.

	RI	SI	N	SW	RW	Tot
Tot samples	68	333	535	114	26	1076
Samples with hot towers	31	122	145	21	3	322
Samples without hot towers	37	211	390	93	22	754
Probabilities (%) of intensity changes for samples without hot towers	4.9	28.0	51.7	12.3	3.1	100
Probabilities (%) of intensity changes for samples with hot towers	9.6	38.0	45.0	6.5	0.9	100
Climatological probabilities (%) of intensity changes	6.3	31.0	49.7	10.6	2.4	100

significant differences of 3 out of 4 convective intensity parameters in the inner core exist between RI and non-RI storms. Between RI and slowly intensifying TCs, statistically significant difference exists for the minimum T_{B11} (note that anvil contamination has been removed, please see section 2b for details) in the inner core. This indicates that a relationship does exist between inner-core convective intensity and TC intensity change. Hendricks et al. (2010) suggests that the environmental differences between rapidly intensifying and slowly intensifying TCs are rather subtle, and RI is more likely controlled by internal processes. The results in this study also suggest that the rate of intensification appears to be influenced by convective activity in the inner core and our ability to predict RI might be further improved by using convective parameters.

With regard to different convective proxies, the relationships are different. The minimum T_{B11}, upper-level maximum radar reflectivities, and maximum 20-dBZ radar echo height in the inner core are best associated with the rate of TC intensity change, while the minimum 85-GHz PCT show some ambiguities in relation to intensity change. The minimum 37-GHz PCT shows no significant relationship with TC intensity change, probably due to the contamination of the ice scattering signal by emission from rain and liquid water in this channel.

By examining the probability of RI for each convective parameter for which statistically significant differences at 95% level were found of RI and non-RI cases, it is found that all the three parameters provide additional information relative to climatology. The most skillful parameter is minimum T_{B11}, and the second is the maximum 20-dBZ height, followed by the minimum 85-GHz PCT. However, the increases of RI probability from the larger sample mean by using these predictors are not very large.

When using a hot tower as a predictor, it is found that the probabilities of RI and slowly intensifying increase and those of slowly weakening and rapidly weakening decrease for samples with hot towers in the inner core. However, the increases for intensifying and decreases for weakening are not substantial, indicating that hot towers are neither a necessary nor a sufficient condition for RI.

Being only 2.4% of the total sample, the rapidly weakening group represents the most distracting factor for predicting RI using inner-core convective intensity parameters. Since nearly half of rapidly weakening storms are category 3–5 hurricanes, while almost no major hurricane experiences RI, these rapidly weakening cases can be easily differentiated from RI storms. However, the most uncertainty comes from category 1–2 hurricanes, which have almost equal chances of either undergoing rapid intensification or rapid weakening (Table 2). The necessary conditions for rapidly intensifying and rapidly weakening storms are nearly the same (i.e., the maximum 20-dBZ echo height in the inner core must be higher than 7–8 km and the minimum 85-GHz PCT in the same region must be colder than 250 K). Since the differentiation is mainly related to the storm initial intensity, a further examination will be done by separating these two groups into different initial intensity subcategories. A much larger dataset is required to do this.

Although this work assesses the relationship between TC intensity change and convective intensity in the inner core by using global TC data, individual basins are examined for comparisons. Because of the sample size limitation for RI and RW categories in individual basins, only slowly intensifying cases are compared with the neutral (N) and slowly weakening (SW) cases. It is found that there may be significant variability in the global results between individual basins. Three possible scenarios may explain the basin variability: 1) sampling issues of the TRMM data may artificially increase or decrease the true basin average by altering the distribution of convective intensity observations among the different TC intensity classes in each basin; 2) best-track quality is different for different basins, and 3) differences in the TC–environment interactions in each basin may alter the distribution of convective intensity in inner-core PFs associated with intensity changes. Further research is needed to determine the true reason.

This study focuses on examining the point measure of the most intense convective intensity in the inner core. The storm internal processes also include the storm total parameters, such as total volumetric rain and total raining area in the inner core, which are all related to the total latent heat release. Studies in this vein are being done separately using the TRMM TCPF database (Ramirez 2010).

Acknowledgments. The author acknowledges Ed Zipser, Dan Cecil, and Chuntao Liu for their support for this work. The author would also like to give acknowledgments to John Kaplan and another anonymous reviewer for their helpful comments. Support for this study is provided by the NASA Precipitation Measurement Mission (PMM) Grant NNX10AE28G, NASA New Investigator Program (NIP) Grant NNX10AG55G, and NASA Hurricane Science Research Program (HSRP) Grant NNX10AG34G. The authors thank Ramesh Kakar and Ming-Ying Wei (NASA headquarters) for their continued support of TRMM/PMM and hurricane sciences.

REFERENCES

Awaka, J., T. Iguchi, and K. Okamoto, 1998: Early results on rain type classification by the Tropical Rainfall Measuring Mission (TRMM) precipitation radar. *Proc. Eighth URSI Commission F Open Symp.,* Aveiro, Portugal, International Union of Radio Science, 143–146.

Cecil, D. J., and E. J. Zipser, 1999: Relationships between tropical cyclone intensity and satellite-based indicators of inner core convection: 85-GHz ice-scattering signature and lightning. *Mon. Wea. Rev.,* **127,** 103–123.

——, ——, and S. W. Nesbitt, 2002: Reflectivity, ice scattering, and lightning characteristics of hurricane eyewalls and rainbands. Part I: Quantitative description. *Mon. Wea. Rev.,* **130,** 769–784.

——, S. J. Goodman, D. J. Boccippio, and E. J. Zipser, 2005: Three years of TRMM precipitation features. Part I: Radar, radiometric, and lightning characteristics. *Mon. Wea. Rev.,* **133,** 543–566.

DeMaria, M., and J. Kaplan, 1994: A Statistical Hurricane Intensity Prediction Scheme (SHIPS) for the Atlantic basin. *Wea. Forecasting,* **9,** 209–220.

——, and ——, 1999: An updated Statistical Hurricane Intensity Prediction Scheme (SHIPS) for the Atlantic and eastern North Pacific basins. *Wea. Forecasting,* **14,** 326–337.

Gray, W. M., 1968: Global view of the origin of tropical disturbances and storms. *Mon. Wea. Rev.,* **96,** 669–700.

Guimond, S. R., G. M. Heymsfield, and F. J. Turk, 2010: Multiscale observations of Hurricane Dennis (2005): The effects of hot towers on rapid intensification. *J. Atmos. Sci.,* **67,** 633–654.

Hendricks, E. A., M. T. Montgomery, and C. A. Davis, 2004: The role of ''vortical'' hot towers in the formation of Tropical Cyclone Diana (1984). *J. Atmos. Sci.,* **61,** 1209–1232.

——, M. S. Peng, B. Fu, and T. Li, 2010: Quantifying environmental control on tropical cyclone intensity change. *Mon. Wea. Rev.,* **138,** 3243–3271.

Iguchi, T., T. Kozu, R. Meneghini, J. Awaka, and K. Okamoto, 2000: Rain-profiling algorithm for the TRMM Precipitation Radar. *J. Appl. Meteor.,* **39,** 2038–2052.

Jiang, H., C. Liu, and E. J. Zipser, 2011: A TRMM-based tropical cyclone cloud and precipitation feature database. *J. Appl. Meteor. Climatol.,* **50,** 1255–1274.

Kaplan, J., and M. DeMaria, 2003: Large-scale characteristics of rapidly intensifying tropical cyclones in the North Atlantic basin. *Wea. Forecasting,* **18,** 1093–1108.

——, ——, and J. A. Knaff, 2010: A revised tropical cyclone rapid intensification index for the Atlantic and eastern North Pacific basins. *Wea. Forecasting,* **25,** 220–241.

Kelley, O. A., J. Stout, and J. B. Halverson, 2004: Tall precipitation cells in tropical cyclone eyewalls are associated with tropical cyclone intensification. *Geophys. Res. Lett.,* **31,** L24112, doi:10.1029/2004GL021616.

——, ——, and ——, 2005: Hurricane intensification detected by continuously monitoring tall precipitation in the eyewall. *Geophys. Res. Lett.,* **32,** L20819, doi:10.1029/2005GL023583.

Kerns, B., and E. J. Zipser, 2009: Four years of tropical ERA-40 vorticity maxima tracks. Part II: Differences between developing and nondeveloping disturbances. *Mon. Wea. Rev.,* **137,** 2576–2591.

Liu, C., E. J. Zipser, and S. W. Nesbitt, 2007: Global distribution of tropical deep convection: Different perspectives from TRMM infrared and radar data. *J. Climate,* **20,** 489–503.

——, ——, D. J. Cecil, S. W. Nesbitt, and S. Sherwood, 2008: A cloud and precipitation feature database from 9 years of TRMM observations. *J. Appl. Meteor. Climatol.,* **47,** 2712–2728.

Merrill, R. T., 1988: Environmental influences on hurricane intensification. *J. Atmos. Sci.,* **45,** 1678–1687.

Montgomery, M. T., M. E. Nicholls, T. A. Cram, and A. B. Saunders, 2006: A vortical hot tower route to tropical cyclogenesis. *J. Atmos. Sci.,* **63,** 355–386.

Nesbitt, S. W., E. J. Zipser, and D. J. Cecil, 2000: A census of precipitation features in the tropics using TRMM: Radar, ice scattering, and lightning observations. *J. Climate,* **13,** 4087–4106.

Ramirez, E. M., 2010: Convective and rainfall properties of tropical cyclone inner cores and rainbands in relation to tropical cyclone intensity changes using 12 years of TRMM data. M.S. thesis, Dept. of Atmospheric Sciences, University of Utah, 134 pp.

Rao, G. V., and P. D. MacArthur, 1994: The SSM/I estimated rainfall amounts of tropical cyclones and their potential in predicting the cyclone intensity changes. *Mon. Wea. Rev.,* **122,** 1568–1574.

Rogers, R., 2010: Convective-scale structure and evolution during a high-resolution simulation of tropical cyclone rapid intensification. *J. Atmos. Sci.,* **67,** 44–70.

Simpson, J., J. B. Halverson, B. S. Ferrier, W. A. Peterson, R. H. Simpson, R. Blakeslee, and S. L. Durden, 1998: On the role of ''hot towers'' in tropical cyclone formation. *Meteor. Atmos. Phys.,* **67,** 15–35.

Spencer, R. W., H. M. Goodman, and R. E. Hood, 1989: Precipitation retrieval over land and ocean with the SSM/I: Identification and characteristics of the scattering signal. *J. Atmos. Oceanic Technol.,* **6,** 254–273.

Steranka, J., E. B. Rodgers, and R. C. Gentry, 1986: The relationship between satellite measured convective bursts and tropical cyclone intensification. *Mon. Wea. Rev.,* **114,** 1539–1546.

Szoke, E. J., and E. J. Zipser, 1986: A radar study of convective cells in mesoscale systems in GATE. Part II: Life cycles of convective cells. *J. Atmos. Sci.,* **43,** 199–218.

Vigh, J. L., and W. H. Schubert, 2009: Rapid development of the tropical cyclone warm core. *J. Atmos. Sci.,* **66,** 3335–3350.

Vivekanandan, J., J. Turk, and V. N. Bringi, 1991: Ice water path estimation and characterization using passive microwave radiometry. *J. Appl. Meteor.,* **30,** 1407–1421.

Zipser, E. J., and K. R. Lutz, 1994: The vertical profile of radar reflectivity of convective cells: A strong indicator of storm intensity and lightning probability? *Mon. Wea. Rev.,* **122,** 1751–1759.

——, D. J. Cecil, C. Liu, S. W. Nesbitt, and D. P. Yorty, 2006: Where are the most intense thunderstorms on earth? *Bull. Amer. Meteor. Soc.,* **87,** 1057–1071.